Perpendicular upper critical field of superconducting—normal-metal multilayers

Kevin R. Biagi, Vladimir G. Kogan, and John R. Clem
Ames Laboratory and Department of Physics, Iowa State University, Ames, Iowa 50011
(Received 8 July 1985)

An equation is derived for the upper critical field, $H_{c2}(T)$, perpendicular to superconductor—normal-metal (SN) multilayers. The theoretical $H_{c2}(T)$ agrees with experimental data for Nb-Cu multilayers only if the mean free paths of both S and N metals are considerably smaller than the estimates obtained from longitudinal resistivity measurements. Positive curvature in $H_{c2}(T)$ near the critical temperature is reproduced by the theory. Field-dependent corrections to the pair penetration depth into the N metal are shown to enhance $H_{c2}(T)$.

I. INTRODUCTION

Multilayered superconductors range from intercalated compounds to artificially layered structures. They commonly consist of alternating superconducting (S) layers separated by a variety of different materials, e.g., insulators, normal metals (N), or other superconductors. In this paper we focus on the upper critical field $H_{c2}(T)$ normal to SN multilayers.

First attempts to calculate the upper critical-field treated layered compounds as a stack of two-dimensional superconductors coupled via the Josephson effect.[1–4] This model disregards any variation of the order parameter in the direction z, perpendicular to the layers. However, as the layer thickness increases with respect to the coherence length, the z variation of the order parameter is no longer negligible. Since this is generally the case for all but the thinnest SN multilayers, proximity effects must be taken into account.

Several authors have considered these effects in calculating H_{c2}. Dobrosavljevic[5] used the anisotropic Ginzburg-Landau (GL) equations and treated the multilayered system as a single, composite superconductor. Nabutovskii and Shapiro (see Ref. 6 and references therein) developed a microscopic theory for various types of inhomogeneous superconductors, including multilayers. A similar approach was used by Menon and Arnold[7] for dirty bimetallic superlattices. In both Refs. 6 and 7 the individual layers were assumed to differ only in their respective electron-phonon coupling constants.

A more realistic approach to the problem was suggested by Ruggiero, Barbee, and Beasley,[8] who also accounted for differences in diffusivities and densities of states at the Fermi levels of the S and N layers. Essentially the same problem has been considered by Martinoli for an SN bilayer.[9] These authors started with the equation given by de Gennes, Werthamer, and co-workers[10] for the critical temperature of a dirty SN bilayer and used pair-breaking arguments to infer the correct form of the equation determining $H_{c2}(T)$. The discussion in Ref. 8 is restricted to the GL domain; no comparison of the theoretical results for a multilayer with experimental $H_{c2}(T)$ data is reported.

Recently, Tachiki and Takahashi[11] reported H_{c2} calculations based on de Gennes's approach. These authors were able to evaluate, in the dirty limit, both parallel and perpendicular H_{c2}'s and to reproduce the main observed features of these fields. However, a detailed comparison with the experimental data still remains to be done.

We present here a theory for the perpendicular upper critical field based on Eilenberger's quasiclassical description of superconductivity.[12] This formalism is effective in dealing with inhomogeneous superconductors in magnetic fields. No restrictions are placed on either the temperature or the mean free paths l. Although in this work we consider mainly the dirty limit, we are able to go beyond this approximation. In fact, our method can be generalized to arbitrary l's.[13,14] In the dirty limit our result agrees with that given in Ref. 8.

Our work differs from previous publications in a number of ways. We perform a detailed comparison between theory and experiment, which allows us to extract information concerning the mean free paths and the SN interfaces. We demonstrate that positive curvature can exist in theoretical $H_{c2}(T)$ curves under certain conditions. This effect has been observed in a number of experiments,[8,15–17] and several speculations as to its cause have been proposed. It is shown in this work that the proximity effect alone can produce the positive curvature in $H_{c2}(T)$. Finally, we include recent results concerning field-dependent corrections to the pair penetration depth in the N layers.[14]

This paper is organized as follows: In Sec. II we derive an equation for the perpendicular upper critical field. We compare the theory with experimental data for Nb-Cu multilayers in Sec. III. Section IV addresses the topic of positive curvature, while Sec. V deals with corrections to the dirty-limit equations discussed in Sec. II. Finally, we summarize and discuss our results in Sec. VI.

II. DERIVATION OF THE MAIN EQUATION

We start with the dirty-limit version of the Eilenberger theory[18]

$$-\frac{D}{2}\Pi\cdot(G\Pi F-F\nabla G)=\frac{\Delta}{\hbar}G-\omega F\ , \tag{1}$$

$$G^2+|F|^2=1\ , \tag{2}$$

and

$$\Delta \ln\frac{T_c}{T}=2\pi T\sum_{\omega}\left[\frac{\Delta}{\hbar\omega}-F\right] . \tag{3}$$

Here, $D=vl/3$ is the diffusion coefficient with v being the Fermi velocity. The temperature T has units of energy, $\hbar\omega=\pi T(2n+1)$ with $n=0,1,2,\ldots$, and $\Pi=\nabla+2\pi i\mathbf{A}/\phi_0$ is the gauge-invariant gradient with vector potential $\mathbf{A}$ and flux quantum ϕ_0. The pair potential $\Delta(\mathbf{r})$ depends only upon position $\mathbf{r}$ as required for a superconductor with weak coupling. The functions $F(\mathbf{r},\omega)$ and $G(\mathbf{r},\omega)$ are Gorkov's Green's functions integrated over energy and averaged over the Fermi surface. They describe the condensate of pairs and the normal excitations, respectively. Maxwell's equations, along with an expression for the current density,[18] complete this set but are not used in this paper.

In the normal state, $F=0$ and $G=1$. Near the second-order phase transition at $H_{c2}(T)$, $|F|\ll 1$ and $G=1$ in the approximation linear in F. Equation (1) now can be linearized:

$$-\frac{D}{2}\Pi^2F=\frac{\Delta}{\hbar}-\omega F . \tag{4}$$

This must be solved in conjunction with the self-consistency condition (3).

Since both $F(\mathbf{r},\omega)$ and $\Delta(\mathbf{r})$ vanish at $H_{c2}(T)$, we seek a solution to Eqs. (3) and (4) of the form $F(\mathbf{r})=\Delta(\mathbf{r})/[\hbar\omega+\pi Ty(t)]$ with the reduced temperature $t=T/T_c$. Here, T_c represents the bulk critical temperature of either metal, i.e., T_{cs} or T_{cn} (the subscripts s and n refer to the S and N layers, respectively, and N denotes the metal with the lowest critical temperature). With this ansatz Eq. (4) reduces to

$$\Pi^2F=-k^2F \tag{5}$$

with

$$k^2=2\pi Ty(t)/\hbar D . \tag{6}$$

Note that Eq. (5) is formally identical to the linearized GL equation for the order parameter but holds at any T (at H_{c2}).

Equation (3), which defines $y(t)$, becomes

$$\ln t=-2\sum_{n=0}^{\infty}\left[\frac{1}{2n+1}-\frac{1}{2n+1+y}\right] \tag{7}$$

or

$$\ln t=\psi(\tfrac{1}{2})-\psi(\tfrac{1}{2}+y/2) , \tag{8}$$

where $\psi(x)$ is the digamma function. The sign of $y(t)$ depends upon whether $t<1$ or $t>1$. For S, $t_s=T/T_{cs}<1$ and Eq. (7) implies that $y(t_s)>0$. The "normal-metal" component of the proximity system can itself be a superconductor with a finite critical temperature T_{cn}, such that $0<T_{cn}<T_{cs}$. Thus, $y(t_n)<0$ for $t_n=T/T_{cn}>1$, but $y(t_n)>0$ for $T<T_{cn}$. If $T_{cn}\to 0$, as is the case for Cu, then $y(t_n\to\infty)=-1$.

Caution should be exercised when applying the dirty-limit theory to a normal metal. This limit for the S metal corresponds to a large impurity parameter

$$\lambda_s=\frac{\hbar v_s}{2\pi T_{cs}l_s}\simeq\frac{\xi_s(0)}{l_s}\gg 1 , \tag{9}$$

where $\xi_s(0)$ is the BCS coherence length at $T=0$. This criterion is not applicable to a normal metal with $T_{cn}=0$. Instead, as shown in Ref. 13, the relevant condition for the dirty limit in N is

$$\lambda_n=\frac{\hbar v_n}{2\pi Tl_n}\gg 1 . \tag{10}$$

Observe that the parameter λ_n is inversely proportional to temperature. As a consequence, normal metals such as Cu considered "clean" at some T become "dirty" at low enough temperatures. Therefore, to apply the dirty-limit theory, the criterion (10) must be satisfied at the highest T considered (T_{csn} in our case).

A more general approach is required if conditions (9) and (10) are not satisfied. This situation is discussed in Ref. 14, where it is shown that Eq. (5) is still valid, but the corresponding expression for k differs significantly from Eq. (6). The most interesting result of this analysis is the field dependence of k, which is field independent in the dirty limit or in the GL domain. We will return to the H-independent corrections to the dirty limit k in Sec. V.

Now consider an infinite stack of alternating S and N layers, which are parallel to the x-y plane with a period of d_s+d_n, where $d_{s,n}$ are the thicknesses of the S and N layers. The coordinates are chosen so that $z=0$ defines the SN interface of the elementary cell $-d_n\le z\le d_s$. For a uniform magnetic field $\mathbf{H}=H\hat{\mathbf{z}}$, we use the gauge $A_x=A_z=0$ and $A_y=Hx$; the gauge-invariant gradient becomes

$$\Pi=\left[\frac{\partial}{\partial x},\frac{\partial}{\partial y}+2\pi iHx/\phi_0,\frac{\partial}{\partial z}\right] .$$

Then the z variable in Eq. (5) can be separated: $F(x,y,z)=f(x,y)g(z)$. We obtain for f and g

$$-(\Pi_x^2+\Pi_y^2)f_s(x,y)=(k_s^2-q_s^2)f_s(x,y) , \tag{11a}$$

$$g_s''(z)=-q_s^2g_s(z) \tag{11b}$$

for the S layers and

$$-(\Pi_x^2+\Pi_y^2)f_n(x,y)=(-k_n^2+q_n^2)f_n(x,y) , \tag{12a}$$

$$g_n''(z)=q_n^2g_n(z) \tag{12b}$$

for the N layers. Here, $q_{s,n}$ are separation constants and $k_{s,n}$ are defined by

$$k_s^2=2\pi Ty(t_s)/\hbar D_s \tag{13a}$$

and

$$k_n^2=-2\pi Ty(t_n)/\hbar D_n . \tag{13b}$$

Equations (11) and (12) are subject to certain boundary conditions at SN interfaces.[19] For a sharp boundary at $z=0$,

$$F_s=F_n \tag{14a}$$

and

$$\frac{\partial F_s}{\partial z}=\eta\frac{\partial F_n}{\partial z}\ . \tag{14b}$$

The parameter η characterizes the interfaces. For specular scattering in the dirty limit, $\eta=\sigma_n/\sigma_s$, with σ standing for normal conductivities. Equations (14) are satisfied if

$$g_s(0)=g_n(0) \tag{15a}$$

and

$$g_s'(0)=\eta g_n'(0)\ , \tag{15b}$$

whereas $f_s(x,y)$ and $f_n(x,y)$ must be identical. Hence the eigenvalues of Eqs. (11a) and (12a) are also identical: $k_s^2-q_s^2=-k_n^2+q_n^2$.

Equations (11a) and (12a) are equivalent to the Schrödinger equation for a charged particle in a uniform magnetic field. The lowest eigenvalue $2\pi H/\phi_0$ gives the largest field H_{c2} for which a finite solution exists in the whole x-y plane. We then obtain

$$q_s^2=k_s^2-2\pi H_{c2}/\phi_0 \tag{16a}$$

and

$$q_n^2=k_n^2+2\pi H_{c2}/\phi_0\ . \tag{16b}$$

Note that $q_s^2>0$ when $H_{c2}<H_{c2,s}$, where $H_{c2,s}=\phi_0 k_s^2/2\pi$ is the bulk upper critical field of the S material.

Equations (11a) and (12a) yield a system of Abrikosov vortices, which are modulated in the z direction by $g_{s,n}(z)$. From Eqs. (11b) and (12b) we obtain

$$g_s(z)=C_s\cos[q_s(z-d_s/2)] \tag{17}$$

and

$$g_n(z)=C_n\cosh[q_n(z+d_n/2)]\ , \tag{18}$$

where C_s and C_n are arbitrary constants. By writing the solutions in this form we account for the multilayer symmetry planes at $z=d_s/2$ and $z=-d_n/2$. It is worth noting that Eq. (18) implies that q_n^{-1} is the characteristic "pair penetration depth" in the N layers in our geometry. Boundary conditions (15) now yield two linear homogeneous equations for C_s and C_n. After setting the determinant equal to zero, we obtain[8]

$$q_s\tan(q_s d_s/2)=\eta q_n\tanh(q_n d_n/2)\ . \tag{19}$$

When combined with Eqs. (8), (13), and (16), this equation completely determines $H_{c2}(T)$. In general, this must be done numerically.

At the multilayer critical temperature T_{csn}, $H_{c2}=0$ and $q_{s,n}^2=k_{s,n}^2$. Equation (19) reduces to the result of de Gennes, Werthamer, and co-workers[10] for the critical temperature of a dirty SN proximity system. In fact, the equations explored in Ref. 10 are the same as Eq. (5). Although the function used by Werthamer, which we call $F_W(\mathbf{r})$, differs from our $F(\mathbf{r},\omega)$, the two functions are closely related:

$$F_W(\mathbf{r})=2\pi TN(0)\sum_{\omega}F(\mathbf{r},\omega)\ , \tag{20}$$

with $N(0)$ being the density of states at the Fermi level. Both approaches yield the same critical temperature if de Gennes's boundary conditions of continuity for $F_W/N(0)$ and DF_W' are replaced in our case by continuity of F and $DN(0)F'$ (Ref. 19). Thus, the theory of $H_{c2}(T)$ presented here is equivalent to the de Gennes–Werthamer theory generalized to include the presence of a magnetic field.

In the limit $d_s\to\infty$ or $d_n\to 0$, Eq. (19) gives $H_{c2}=H_{cs,s}$, as expected. A more interesting simple case is when both $k_s d_s\ll 1$ and $k_n d_n\ll 1$. In this limit, Eq. (19) reduces to

$$H_{c2}=\frac{H_{c2,s}(T)}{1+\eta d_n/d_s}\left[1-\eta\frac{d_n k_n^2}{d_s k_s^2}\right]\ . \tag{21}$$

Note that $k_n=0$ at $T=T_{cn}$, so that if $T_{cn}=0$,

$$H_{c2}(0)=\frac{H_{c2,s}(0)}{1+\eta d_n/d_s}\ . \tag{22}$$

An expression for the slope dH_{c2}/dT evaluated at $T=T_{csn}$ is given in the Appendix.

III. COMPARISON WITH EXPERIMENT

In order to test the theory presented in Sec. II, we use $H_{c2}(T)$ data for Nb-Cu multilayers obtained in Refs. 17 and 20. These specimens were prepared using a sequential deposition technique that produces layers of equal thickness, $d_s=d_n=d$. In addition, the Nb-Cu system exhibits epitaxial registry between adjacent layers with little interlayer diffusion. In what follows we describe our method for fitting $H_{c2}(T)$ to these data and discuss the results.

A. Fitting parameters and numerical procedure

Calculating $H_{c2}(T)$ from Eq. (19) requires that we specify the quantities T_{cs}, T_{cn}, $d_{s,n}$, $v_{s,n}$, $l_{s,n}$, and η. These parameters control the overall shape and magnitude of the theoretical $H_{c2}(T)$ curves. First consider the critical temperature T_{cn} and T_{cs}, which enter Eq. (23) through Eq. (8). For Cu we assume $T_{cn}=0$, which implies that $k_n^2=2\pi T/\hbar D_n$. The appropriate value for T_{cs} depends upon the S-layer thickness. Banerjee *et al.*[21] observed a large suppression in T_{csn} with decreasing layer thickness which cannot be accounted for by the de Gennes–Werthamer theory. The mechanisms or material properties responsible for this behavior are still not well understood.[22] Instead of using a single bulk value for the T_{cs}, we thus use thickness-dependent values as determined in Ref. 21.

The diffusion coefficients $D_{s,n}=(vl/3)_{s,n}$ influence $H_{c2}(T)$ through k_s and k_n. For the respective Fermi velocities we use the free-electron value $v_n=1.57\times10^8$ cm/sec (Ref. 23) for Cu and a measured root-mean-square value of $v_s=2.73\times10^7$ cm/sec (Ref. 24) for Nb.

Longitudinal resistivity measurements have been interpreted as indicating that the mean free paths are generally layer-thickness limited due to size effects.[25] In Ref. 21, a model was adopted where $l_{s,n}=d_{s,n}$ for thicknesses less than the bulk mean free paths. For thicker layers, it was assumed that boundary scattering is less important and

that the mean free paths are equal to their bulk values. Unfortunately, this simple model yields poor agreement between our theory and experiment. For the cases we examined, the $H_{c2}(T)$ curves calculated using the l_s and l_n of this model fell far below the experimental data. Realistic curves are obtained only when the mean free paths, particularly l_s, are significantly smaller than both $d_{s,n}$ and the bulk mean free paths estimated in Ref. 21.

For this reason, instead of evaluating the $H_{c2}(T,l_{s,n})$ with values for $l_{s,n}$ from Ref. 21, we rather consider both l_s and l_n as fitting parameters. Thus, in the following we extract $l_{s,n}$ from the $H_{c2}(T)$ data using Eq. (19) complemented with Eqs. (8), (13), and (16).

Now consider the interfacial boundary condition parameter η defined by Eq. (15b). As mentioned in Sec. II, $\eta=\sigma_n/\sigma_s$ for specular scattering, but actual physical properties of interfaces are usually unknown. To account for this uncertainty, we observe that $\sigma_n/\sigma_s \propto l_n/l_s$, so that it is reasonable to assume that

$$\eta=\alpha l_n/l_s \ , \tag{23}$$

where we have introduced the dimensionless parameter α. For purposes of comparison, note that $\alpha_0=N_n(0)v_n/N_s(0)v_s$ for perfectly specular scattering. As with the mean free paths, α is determined by fitting $H_{c2}(T)$ to experimental data.

The fitting procedure involves minimizing

$$\chi^2(l_s,l_n,\alpha)=\sum_{i=1}^{n}[\delta H_{c2}(T_i)]^2 \tag{24}$$

with respect to l_s, l_n, and α. The quantity $\delta H_{c2}(T_i)$ is the difference between the measured and calculated values of $H_{cs}(T)$ at temperature T_i, and n is the number of data points:

$$\delta H_{c2}(T_i)=H_{c2}^{\rm expt}(T_i)-H_{c2}(T_i;l_s,l_n,\alpha) \ .$$

The minimization of χ^2 is achieved by using a standard simplex algorithm.[26] This method involves no derivatives and converges even with poor initial guesses. The values of l_s, l_n, and α for which χ^2 is an absolute minimum, are then used to calculate $H_{c2}(T)$.

B. Results

We now examine two representative Nb-Cu multilayers. The first one is of thickness $d=d_s=d_n=420.5$ Å and with $T_{cs}=8.91$ K.[21] The resulting parameters are listed in the first three columns of Table I. In Fig. 1(a) both the theoretical curve and the experimental data are plotted as a function of the reduced temperature $t_s=T/T_{cs}$. The fit is good and spans the entire temperature range. Upon close inspection we observe slight positive curvature near T_{csn} in both the experimental and theoretical curves. This is demonstrated in Fig. 1(b), where we plot the second derivative of the theoretical curve shown in Fig. 1(a). The subject of positive curvature is discussed in detail in Sec. IV.

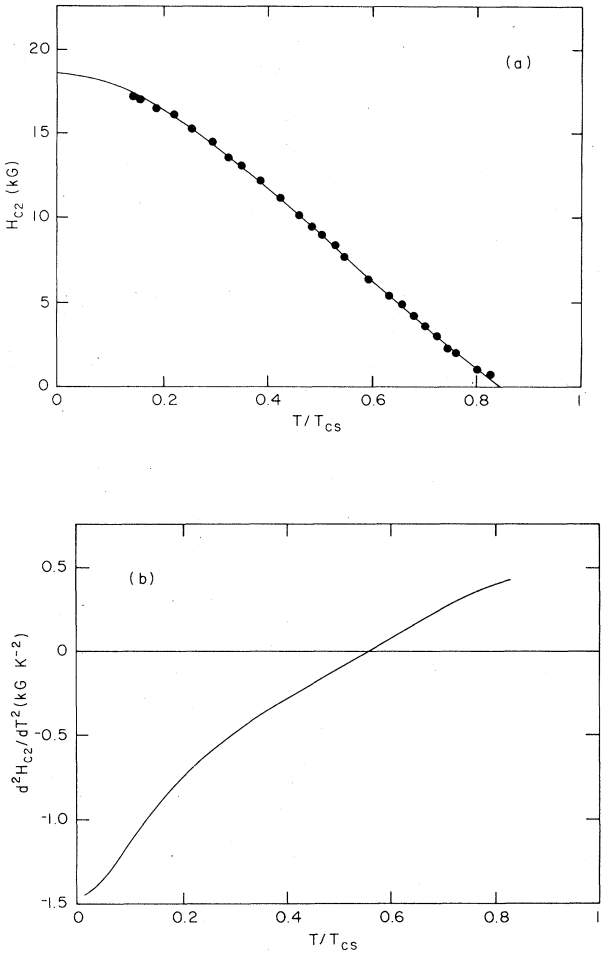

FIG. 1. (a) Upper critical field H_{c2} vs T/T_{cs} for $d=420.5$ Å. The points are experimental data and the solid curve was calculated from Eq. (19) using the "field-independent" parameters listed in Table I. (b) Second derivative $H_{c2}''(T)$ of the theoretical curve in (a).

The fit to data for $d=171.5$ Å was performed using $T_{cs}\simeq 8.4$ K (Ref. 21), and the resulting parameters are given in Table I. The theoretical curve and the experimental data are shown in Fig. 2. The fit to the data is

TABLE I. Fitting parameters for Nb-Cu multilayers for experimental results of Ref. 17.

	Field-independent k_n			Field-dependent k_n		
d (Å)	l_n (Å)	l_s (Å)	α	l_n (Å)	l_s (Å)	α
420.5	113	24	0.68	104	26	0.64
171.5	96	14	0.76	84	21	0.69

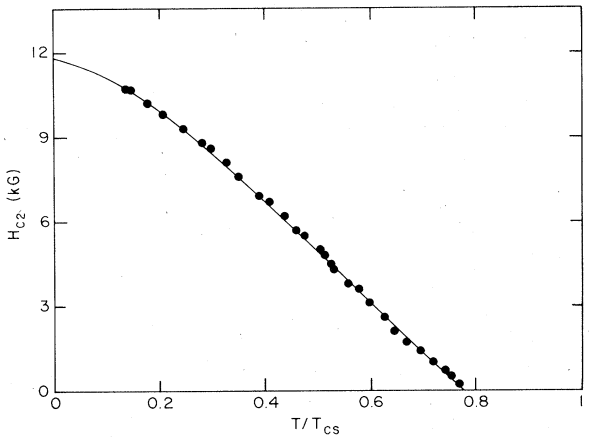

FIG. 2. Upper critical field H_{c2} vs T/T_{cs} for $d=171.5$ Å.

also good, but in this case the theoretical curve does not show any appreciable positive curvature.

The mean free paths obtained from these fits are all significantly smaller than the layer thicknesses and the bulk mean free paths estimated in Ref. 21 ($l_s \simeq 160$ Å, $l_n \simeq 2000$ Å). This discrepancy is not unique to the samples discussed; similar results were obtained for all the Nb-Cu multilayers we examined.

In order to interpret our values for α we compare them with

$$\alpha_0 = N_n(0)v_n / N_s(0)v_s = \gamma_n v_n / \gamma_s v_n ,$$

where $\gamma_{s,n}$ are the normal-state electronic specific-heat coefficients. Using $\gamma_n = 0.693$ mJ/mol K^2 and $\gamma_s = 7.66$ mJ/mol K^2 (Ref. 27), we obtain $\alpha_0 = 0.76$ as compared to 0.68 and 0.76 needed to fit the theory to the data. Thus these values are in good agreement with what one would expect for specular interfacial scattering.

IV. POSITIVE CURVATURE

Positive curvature (PC) in $H_{c2}(T)$ is a feature common to multilayered superconductors.[8,15–17] Several explanations for the presence of PC have been proposed, but most are difficult to confirm or to deal with quantitatively. Two proposed sources of PC are compositional inhomogeneities and Fermi surface anisotropy. A detailed discussion of these and other possible effects is given by Haywood and Ast.[15]

Recall that in the derivation of Eq. (19) no provisions were made for anisotropy or any other effects commonly thought to produce PC in $H_{c2}(T)$. Even so, we observe PC in our theoretical curves; e.g., see Fig. 1(b). This indicates that the presence or absence of PC is determined by the complex interplay among the parameters $d_{s,n}$ and $k_{s,n}$.

In Fig. 1(b) we see that the curvature is a maximum at T_{csn}. Therefore it is convenient to characterize the amount of curvature via the value $H_{cs}'' \equiv d^2H_{c2}/dT^2$ at the critical temperature T_{csn}. Using Eq. (19) to obtain $H_{c2}''(T_{csn})$, we can examine its behavior as different parameters are varied. The following calculations were performed using $l_n = 100$ Å, $l_s = 20$ Å, and $\alpha = 0.7$, which are representative of the Nb-Cu multilayers discussed in Sec. III.

In Fig. 3 we show $H_{c2}''(T_{csn})$ as a function of d_n for a series of thicknesses d_s. For each value of d_s, $H_{c2}''(T_{csn})$ increases steadily with d_n, reaching a maximum before gradually leveling off. For $d_n > 3000$ Å, $H_{c2}''(T_{csn})$ saturates and becomes independent of d_n. Saturation is expected in a proximity system when d_n is considerably larger than the pair penetration depth q_n^{-1} in N. If instead $d_n \to 0$, the system behaves as a bulk superconductor and exhibits no PC. Thus all the curves shown in Fig. 3 approach the same negative value as $d_n \to 0$, the bulk value,[28] although this is not shown in the figure. The overall trend is clear: decoupling the superconducting layers by increasing their separation d_n enhances the PC. This observation is in qualitative agreement with experimental results,[8,16] although, to our knowledge, no confirmation has been reported for the maxima predicted in our curves.

In Fig. 4 we plot $H_{c2}''(T_{csn})$ as a function of d_s for different thicknesses d_n. As $d_s \to \infty$, each curve descends and eventually saturates at the same negative value[28] for the bulk S. This is equivalent to letting $d_n \to 0$ for finite d_s.

We carried our further calculations to determine the conditions that enhance PC. We used the simplex algorithm[26] to find the d_s and d_n that maximize $H_{c2}''(T_{csn})$ for fixed l_s and l_n. For l_s in the range 10—50 Å and l_n in the range 50—400 Å, $H_{c2}''(T_{csn})$ is maximized when d_s and d_n are two or three times as large as the corresponding lengths k_s^{-1} and k_n^{-1} or, more precisely, when $2.0 < k_s d_s < 2.8$, $2.2 < k_n d_n < 3.1$, and $1.4 < d_n/d_s < 1.6$.

Additional calculations show that $H_{c2}''(T_{csn})$ is also very sensitive to the mean free paths l_s and l_n. For instance, decreasing l_s with l_n constant produces a sharp increase in the PC, chiefly because $H_{c2}''(T_{csn})$ scales with the magnitude of $H_{c2,s}$, which also increases for decreasing l_s. If we fix l_s and increase l_n, the PC increases gradually. This enhancement is the greatest when $l_s \ll l_n$. How-

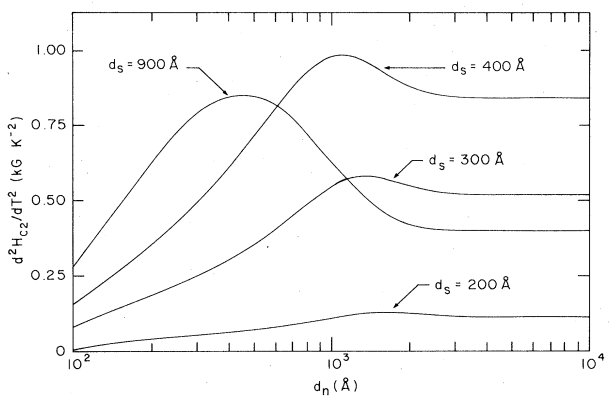

FIG. 3. The second derivative $H_{c2}''(T_{csn})$ as a function of d_n for different values of d_s.

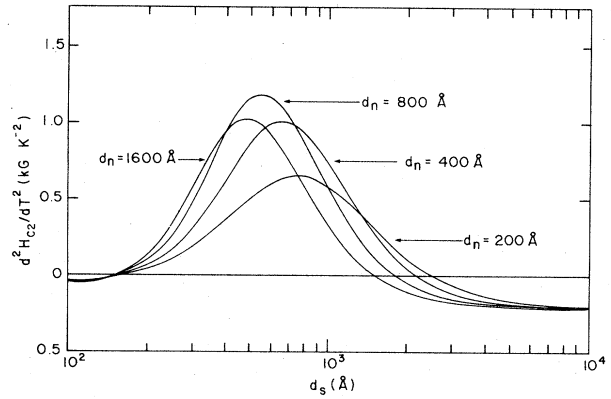

FIG. 4. The second derivative $H_{cs}''(T_{csn})$ as a function of d_s for different values of d_n.

ever, for any thicknesses $d_{s,n}$, $H_{c2}''(T_{csn})$ always can be reduced to zero by reducing l_n or increasing l_s.

These results indicate that PC in $H_{c2}(T)$ is an inherent trait of Eq. (19) and of the T dependencies of $k_{s,n}$. Consequently, a proximity-effect theory for *SN* multilayers is capable of producing PC consistent with experimental results, even in the absence of compositional inhomogeneities or Fermi-surface anisotropy.

V. EFFECTS OF FIELD-DEPENDENT $k_{s,n}$

We now consider how $H_{cs}(T)$ is affected by the field-dependent corrections to k_s and k_n mentioned in Sec. II. If conditions (9) and (10) are not satisfied, then Eqs. (8) and (13) are no longer appropriate. This is the subject of Ref. 14, where corrections to the dirty-limit formulas are obtained. Although Eq. (5) is shown still to be valid, both k_s and k_n are generally no longer field independent.

The relative importance of these corrections differs considerably for the S and N components. The maximum correction to k_s occurs for $T=0$ in the clean limit and cannot exceed roughly 30%. In addition, the impurity parameter $\lambda_s \gg 1$ for the multilayers discussed in Sec. III. As a result, the corrections to k_s are negligible and Eq. (13) suffices.

However, this is not the case for k_n. Even though λ_n of Eq. (10) might be large [for the samples discussed above $\lambda_n(T_{csn}) \simeq 25$], another effect arises due to the field dependence of k_n given by[14]

$$k_n^2(H,T)=k_n^2(0,T)\beta_n^2(1-H^2/H_0^2) . \tag{25}$$

Here, $k_n^2(0,T)=2\pi T/\hbar D_n$ for $T_{cn}=0$; $\beta_n=1+1/\lambda_n$ represents the deviation of the zero field $k_n(0,T)$ from its dirty-limit value and

$$H_0=\frac{\phi_0\beta_n^2}{2\pi l_n^2}\left[\frac{5}{\lambda_n}\right]^{1/2} . \tag{26}$$

Equations (25) and (26) are obtained as a result of an expansion in small parameters $l_n k_n(H)$ and $2\pi l_n^2 H/\phi_0$. The first neglected terms are

$$|k_n^6 l_n^6| \ll 1, \quad |k_n^4 l_n^4| \frac{2\pi H l_n^2}{\phi_0} \ll 1 . \tag{27}$$

Note that $k_n(H_0)=0$. A representative plot of $H_0(T)$ is given by the dashed line in Fig. 5(a). For any l_n, except the limit $l_n \to 0$, $H_{c2}(T)$ inevitably crosses $H_0(T)$ at a finite T, thereby forcing $k_n^2(H,T)$ to change sign.

Using Eqs. (16) and (25), we may express the parameter q_n^2 as

$$q_n^2(H)=k_n^2\beta_n^2+\frac{2\pi H}{\phi_0}-\frac{3}{5}\left[\frac{2\pi H l_n}{\phi_0\beta_n}\right]^2 . \tag{28}$$

The last term here reduces $q_n^2(H)$ with respect to $q_n^2(0)$ obtained with H-independent k_n [Eq. (16)] and, therefore, increases the penetration depth q_n^{-1} in the N layers. This implies that the solution $H_{c2}(T)$ of Eq. (19) will show an overall increase if $k_n(H)$ is used instead of $k_n(0)$. The enhancement is most pronounced at $T=0$. This is demonstrated in Fig. 5(a) where representative $H_{c2}(T)$ curves are shown for both cases. The corresponding $H_{c2}''(T)$ are shown in Fig. 5(b). Note that the field-dependent corrections to k_n enhance the positive curvature at T_{cns}.

Using Eq. (28) instead of Eq. (16) for q_n, we fit $H_{c2}(T)$ to experimental data in the manner described in Sec. III. The resulting best-fit parameters for the two samples considered are given in the last three columns of Table I.

VI. DISCUSSION

In the preceding sections we have presented a theory for $H_{c2}(T)$ of *SN* multilayers based on the proximity effect. This approach yields good agreement between theory and experiment, including the subtle details of positive curvature in $H_{c2}(T)$. However, the mean free paths, and l_s in particular, obtained by fitting $H_{c2}(T)$ to the Nb-Cu data are considerably smaller than the layer thicknesses (see Table I) and the mean free paths estimated in Ref. 21. We therefore conclude that our theory cannot be reconciled with the mean-free-path model of Ref. 21.

It is worth noting here that the inequality $H_{c2}(T) < H_{c2,s}$, which holds when $T_{cn}=0$, imposes an upper limit on l_s. For example, a typical value of $H_{c2}(0) \simeq 18$ kG at $T=0$ yields

$$l_s < 0.84\frac{\phi_0 T_{cs}}{\hbar w_s H_{c2}(0)} \simeq 40 \text{ Å} . \tag{29}$$

Thus, even this upper limit is much smaller than d_s and the estimate of 160 Å given in Ref. 21.

One possible explanation for these results is our underlying assumption of isotropic mean free paths. In a multilayered structure the longitudinal and transverse resistivities can vary significantly, thereby bringing into question our use of bulklike isotropic mean free paths. Transverse resistivity measurements, if possible, would provide valuable information concerning this matter.

New and interesting effects arise due to the field dependence of k_n given by (25). As discussed in Sec. V, this can produce a substantial overall increase in $H_{c2}(T)$; e.g., see Fig. 5. Judging from the parameters given in Table I,

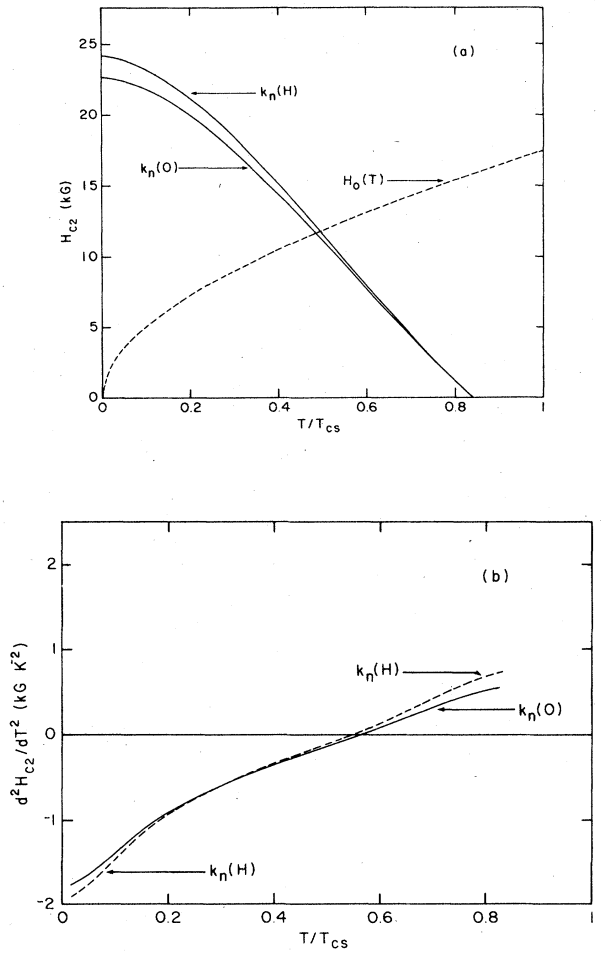

FIG. 5. (a) The upper solid curve is H_{c2} vs T/T_{cs} calculated from Eq. (19) using Eq. (28) with $d_s=d_n=400$ Å, $l_n=100$ Å, $l_s=20$ Å, and $\alpha=0.7$. The dashed curve is $H_0(T)$, where $k_n^2(H)=0$. The lower solid curve corresponds to setting $H=0$ in Eq. (25). (b) Second derivatives $H_{c2}''(T_{csn})$ of the curves in (a).

this effect works to increase the values of l_s needed to fit the data.

The form of the last term in Eq. (28) indicates that the H dependence of k_n has a stronger effect upon $H_{c2}(T)$ when l_n increases. One therefore expects this effect to be more pronounced in clean multilayers. [Note, however, that the theory of Ref. 14 and Eq. (28) are restricted by conditions (27).]

We conclude by noting that the method presented in this paper also can be used to calculate the parallel upper critical field for *SN* multilayers. The approach is essentially the same, although the structure of the superconducting state might be quite different from the two-dimensional array of modulated vortices discussed in this paper.[29] Work along these lines is presently in progress.

ACKNOWLEDGMENTS

The authors wish to thank Dr. Kerry Whisnant for providing the simplex minimization program. Ames Laboratory is operated for the Department of Energy by Iowa State University under Contract No. W-7405-Eng-82. This work was supported by the Director for Energy Research, Office of Basic Energy Science, U. S. Department of Energy.

APPENDIX

The slope dH_{c2}/dT is obtained by differentiating Eq. (19) with respect to T. After setting $T=T_{csn}$, we have

$$\left[\frac{dH_{c2}}{dT}\right]_{T_{csn}}=-2H_{c2,s}\frac{\frac{\gamma_n}{k_n}\frac{dk_n}{dT}-\frac{\gamma_s}{k_s}\frac{dk_s}{dT}}{\gamma_s+\gamma_n\frac{k_s^2}{k_n^2}}, \quad \text{(A1)}$$

with

$$\gamma_s=1+\frac{k_s d_s}{\sin(k_s d_s)},$$

$$\gamma_n=1+\frac{k_n d_n}{\sinh(k_n d_n)},$$

and

$$\frac{dk_{s,n}}{dT}=\frac{k_{s,n}}{2T}\left[1-\left[y\frac{d\psi}{dy}\right]_{s,n}^{-1}\right].$$

Here, $k_{s,n}$ are given by Eqs. (13); Eq. (8) defines $\psi(y)$. If $k_{s,n}d_{s,n}\ll 1$, then $\gamma_{s,n}\to 2$ and Eq. (A1) becomes

$$\left[\frac{dH_{c2}}{dT}\right]_{T_{csn}}=-2H_{c2,s}\frac{\frac{1}{k_n}\frac{dk_n}{dT}-\frac{1}{k_s}\frac{dk_s}{dT}}{1+\frac{k_s^2}{k_n^2}}. \quad \text{(A2)}$$

[1]E. I. Kats, Zh. Eksp. Teor. Fiz. **56**, 1675 (1969) [Sov. Phys.—JETP **29**, 897 (1969)]; **58**, 1471 (1970) [**31**, 787 (1970)].
[2]W. E. Lawrence and S. Doniach, in *Proceedings of the 12th International Conference on Low-Temperature Physics*, edited by E. Kanada (Academic, Kyoto, 1971), p. 361.
[3]L. N. Bulaevskii, Zh. Eksp. Teor. Fiz. **64**, 2241 (1973) [Sov. Phys.—JETP **37**, 1133 (1973)].
[4]R. A. Klemm, M. R. Beasley, and A. Luther, J. Low Temp. Phys. **16**, 607 (1974); R. A. Klemm, A. Luther, and M. R. Beasley, Phys. Rev. B **12**, 877 (1975).
[5]L. Dobrosavljevic, Phys. Status Solidi B **55**, 773 (1973).
[6]V. M. Nabutovskii and B. Ya. Shapiro, J. Low Temp. Phys.

49, 465 (1982).
[7]M. Menon and G. B. Arnold, Superlattices Microstruct. (to be published).
[8]S. T. Ruggiero, T. W. Barbee, and M. R. Beasley, Phys. Rev. B **26**, 4894 (1982).
[9]P. Martinoli, Physica (Utrecht) **55**, 711 (1971); Phys. Kondens. Mater. **16**, 53 (1973); P. Martinoli and J. P. Meraldi, Solid State Commun. **9**, 2123 (1971).
[10]P. G. de Gennes and E. Guyon, Phys. Lett. **3**, 168 (1963); G. Deutscher and P. G. de Gennes, in *Superconductivity,* edited by R. D. Parks (Dekker, New York, 1969), Vol. 2, p. 1005; N. R. Werthamer, Phys. Rev. **132**, 2440 (1963); J. J. Hauser, H. C. Theuerer, and N. R. Werthamer, Phys. Rev. **136**, A637 (1964).
[11]M. Tachiki and S. Takahashi, in Proceedings of the International Conference on Materials and Mechanisms of Superconductivity, Ames, Iowa, 1985 [Physica B (to be published)].
[12]G. Eilenberger, Z. Phys. **214**, 195 (1968).
[13]V. G. Kogan, Phys. Rev. B **26**, 88 (1982).
[14]V. G. Kogan, Phys. Rev. B **32**, 139 (1985).
[15]T. W. Haywood and D. G. Ast, Phys. Rev. B **18**, 2225 (1978).
[16]S. T. Ruggiero, T. W. Barbee, and M. R. Beasley, Phys. Rev. Lett. **45**, 1299 (1980).
[17]I. Banerjee, Ph.D. thesis, Northwestern University, 1982.
[18]K. Usadel, Phys. Rev. Lett. **25**, 507 (1970).
[19]Z. G. Ivanov, M. Yu. Kupriyanov, K. K. Likharev, S. V. Meriakri, and O. V. Snigirev, Fiz. Nizk. Temp. **7**, 560 (1981) [Sov. J.—Low Temp. Phys. **7**, 274 (1981)].
[20]I. Banerjee and I. K. Schuller, J. Low Temp. Phys. **54**, 501 (1984).
[21]I. Banerjee, Q. S. Yang, C. M. Falco, and I. K. Schuller, Solid State Commun. **41**, 805 (1982).
[22]One possible explanation is that $N(0)$ decreases as the mean free path is reduced. Evidence for this is given in Ref. 20, along with a discussion of other effects which can suppress the critical temperature.
[23]N. W. Ashcroft and N. D. Mermin, *Solid State Physics* (Holt, Rinehart, and Winston, New York, 1976), p. 38.
[24]H. R. Kerchner, D. K. Christen, and S. T. Sekula, Phys. Rev. B **24**, 1200 (1981).
[25]T. R. Werner, I. Banerjee, Q. S. Yang, C. M. Falco, and I. K. Schuller, Phys. Rev. B **26**, 2224 (1982); T. R. Werner, Ph.D. thesis, Northwestern University, 1983.
[26]J. A. Nelder and R. Mead, Comput. J. **7**, 308 (1965).
[27]K. A. Gschneidner, in *Solid State Physics,* edited by F. Seitz and D. Turnbull (Academic, New York, 1964), Vol. 16, p. 275.
[28]There is an erroneous statement in the literature that $H_{c2}''(T_c)=0$ in a bulk superconductor (see, e.g., D. E. Prober, R. E. Schwall, and M. R. Beasley, Phys. Rev. B **31**, 2717 (1980). The error stems from misinterpretation of the GL results: $H_{c2}(T\to T_c)\propto(T_c-T)$. However, the corrections to H_{c2} proportional to $(T_c-T)^2$ cannot be obtained in the framework of the GL theory. A simple calculation based on the exact BCS theory of $H_{c2}(T)$ shows that in fact $H_{c2}''(T_c)<0$. In particular, in the dirty limit $H_{c2}''(T_c)=-0.125\phi_0 k_B/\hbar DT_c$, while when $l\to\infty$, $H_{c2}''(T_c)=-26.9\phi_0 k_B^2/\hbar^2 v^2$.
[29]B. Ya. Shapiro, Zh. Eksp. Teor. Fiz. **86**, 68 (1984) [Sov. Phys.—JETP **59**, 120 (1984)].